Nanotechnology Perceptions
ISSN 1660-6795
www.nano-ntp.com

Glaucoma Detection Using Image Denoising and Cascaded UNET Segmentation for Retinal Images

Dr. J. Karunanithi[1], S. Jagadesh Kumar[2]

[1]MCA., M.Phil., Ph.D., Associate Professor and Head, PG & Research Department of Computer Science, Thavathiru Santhalinga Adigalar Arts Science and Tamil College, India
[2]Research Scholar, Department of Computer Applications, Thavathiru Santhalinga Adigalar Arts Science and Tamil College, India

Early glaucoma detection is mandatory for avoiding irreversible visual loss. The important part of glaucoma diagnosis is retinal images, notably fundus images; which provide vital information about the optic disc and cup. Noise prevents these images from exact analysis and diagnosis. To detect glaucoma, this paper proposes Adaptive Noise Elimination Neural Network (ANENN) for image denoising and improved Mask Region-based Convolutional Neural Networks model for segmentation. ANENN utilization is the initial step in correctly removing noise from retinal images. It results in image clarity suitable for further analysis. Next, improved Mask R-CNN model is exploited the cup and optic disc segmentation. This new model uses Mask R-CNN to achieve precise and robust segmentation. In additional, the model exactly estimates Cup-to-Disc Ratio (CDR), an important metric for detecting glaucoma. The presented methodologies outperform the earlier approaches in terms of segmentation accuracy. These methods aids in automated glaucoma screening and earlier detection.

Keywords: Cup-to-Disc Ratio (CDR), Glaucoma detection, Image denoising, Noise removal, Retinal images, Segmentation.

1. Introduction

Glaucoma is a group of eye disease, which permanently damages optic nerve and eventually leads to blindness in case of untreated. It affects millions of people globally and is the leading cause of blindness. Early glaucoma diagnosis preserves vision and helps to prevent further optic nerve damage. Retinal imaging is the primary method for detecting glaucoma because it provides critical information about the eye's optic disc and cup. Optic cup to optic disc ratio is a critical component in determining the severity of glaucoma. Cup-to-Disc Ratio (CDR) is typically within a specific range in healthy eyes. While nerve fiber degenerates, CDR ratio is significantly high in glaucomatous eyes.

Many retinal images still exhibit the same issue of noise added during the process. Limited sensors, motion artifacts and surrounding components are few origins of this noise. Noise lowers the image quality and the gathering of required glaucoma diagnostic features

such as optic disc, optic cup seems challenging. Thus, diminishing the noise is essential to increase retinal imaging quality and improve the automated detection systems.

Image denoising is a common preprocessing technique for medical image analysis. While using denoising techniques like median filtering or Gaussian smoothing, blurring significant visual elements result in incorrect analysis. Optic nerve head and blood vessel components of retinal images render these approaches ineffective. Maintaining such appropriate information is critical for correct segmenting as well as examining optical discs and cups. In medical image denoising, current improvements in Deep Learning (DL)-based algorithms exhibits the accurate results. Important image information is preserved whereas the noise is effectively neglected using Convolutional Neural Networks (CNNs) and adaptive filtering techniques.

After image denoising, segmenting the optic disc and cup comes next in glaucoma detection. Computation of CDR ratio depends on accurate segmentation of these structures. Hence, this is an essential criterion for the diagnosis of glaucoma. For the segmentation techniques like region-growing or thresholding, complex retina architecture, changing image quality and noise provide some difficulties. Deep learning models especially U-Net-based architectures have better performance than the conventional approaches in medical image segmentation tasks by managing image data fluctuations and acquiring sequential features. Being a complete CNN, U-Net is the common choice for biomedical image segmentation. It offers pixel-level accuracy and assist in dividing the minute components like optic disc and cup from the images.

According to this paper, glaucoma is detected in retinal images by proposing a method; in which Adaptive Noise Elimination Neural Network (ANENN) is used for image denoising and Mask Region- based Convolutional Neural Network (Mask R-CNN) for segmentation. Denoising is a noise elimination technique, which improves the image quality by neglecting the noise. Likewise, segmentation is used to divide the optic disk and the cup into two stages. By dealing with segmentation findings and noisy retinal images, the presented approach focus on increasing the overall accuracy of glaucoma detection.

The framework of this paper is that section 2 discusses the various studies on glaucoma detection using segmentation and image denoising. Section 3 elaborates the proposed method. Section 4 illustrates the experimental discussion and results. Section 6 terminates the paper with future work regarding glaucoma detection.

2. BACKGROUND STUDY

Shalini, R., & Gopi, V. P. (2024) proposed a method called Multiresolution Cascaded Attention U-Net (MCAU-Net) that was a Deep Convolutional Neural Networks (CNNs) to precisely localise and segment the OD and fovea structures. Skip connections were made up of cascaded channels and Spatial Attention (SA) modules that allowed the model to accurately target the objects when the convergence was improved during training. Detection of alterations in image and provided accurate local feature extraction along with the lowered image size were improved by the incorporation of wavelet transform. Multipurpose ability of MCAU-Net permitted similar border identification and calculated the image position. The results show that

MCAU-Net handled various dataset sizes and outperformed the state-of-the-art models.

By the utility of Optical Coherence Tomography (OCT) data, Hassan et al. (2021) proposed an automated system called Cascaded Decoupled Convolutional (CDC-Net) for retinopathy evaluation and retinal lesion segmentation. Furthermore, CDC-Net allowed the classification of segmented lesions using a complete and suitable retinopathy grade. CDC-Net was considered as generic model that overlooked the variances in OCT scans from different sources and noise. Categorization and grading of Macular Edema (ME) and Age-Related Macular Degeneration (AMD) retinal pathologies had been presently limited in the proposed CDC-Net approach.

Kang, S., et al. (2021) presented Cascading Modular U-Nets (CMU-Nets), a unique binarization recording approach. CMU-Net with pre-trained modular architecture enabled to function even in the absence of training images. The authors also proposed a novel cascading technique that improved the overall working of cascading models. The proposed model was evaluated on the available Document Image Binarization Competition (DIBCO) and Handwritten-DIBCO (H-DIBCO) datasets.

Lian, S., et al. (2019) introduced the Global and Local enhanced residual U-nEt) approach that used both as globally and locally improved data to monitor the retinal region and precisely segment retinal capillaries. The results of on two benchmark datasets suggest that the presented model was quite successful. In terms of segmentation accuracy, this technique consistently outperformed cutting-edge classical U-Net approaches.

Zhang, Y., et al. (2023) proposed a complete network called TranSegNet. This network developed a hybrid encoder by combining the best features of U-shaped network and lightweight Vision Transformer (ViT). An upgraded U-net backbone yielded CNN characteristics with multiscale resolution. Following that, feature information was collected worldwide using a ViT equipped multi-head convolutional attention. This allowed precise segmentation and localization of retinal layers and damaged tissues. The experimental results showed that hybrid CNN-ViT had reduced computational complexity and parameter size when maintaining the excellent performance. This made it as an efficient encoder for retinal OCT image segmentation applications.

In this work, Aurangzeb, K., et al. (2023) addressed the retinal vascular segmentation using fundus images and suggested a modified form of the ColonSegNet model. This model addressed the problem of inadequate graded images by including data augmentation and efficient methods of locating the real vessels. This work aimed to maximize the contrast of retinal fundus images to the best possible value by means of intelligent evolution algorithms. The presented technique successfully segmented retinal vessels on DRIVE, CHASE_DB, and STARE with high sensitivity, specificity and accuracy ({0.839, 0.979, 0.966}, {0.865, 0.979, 0.971}, and {0.867, 0.981, 0.972}). The development of automated systems for the earliest detection and treatment of eye diseases was an important field for public health improvement.

Yu, Y., et al. (2023) adopted a segmentation-refining network architecture to improve and fine-tune segmentation findings. Initial segmentation network was developed with Multi-scale Multi-structure U-net (M3U), a lightweight encoder-decoder framework. Convolutional Denoising Variational Auto-Encoder (CDVAE) was then utilized to create a refinement

network that improved segmentation results and reduced background noise. This method concluded with Hierarchical Feature Fusion (HFF) unit that combined the intermediate features of segmentation network with pre-segmentation discoveries. To demonstrate the success of the proposed approach, we the results were compared to DRIVE, STARE and HRF datasets.

Mehmood, M., et al. (2024) proposed a lightweight Deep Learning (DL) model based on multitask learning that assisted the clinicians in examining the images of retina. These examinations included the optic disc and retinal artery. The proposed encoder-decoder architecture had captured local, long-range associations from convolutional layers with the utilization of multi-head attention. The features of convolutional layer had combined multi-head attention to improve the model's efficiency and longevity for segmentation tasks. The combined Convolutional Block Attention Module (CBAM) and the decoder skip connections improved the characteristics better. Table 1 compares the different models proposed by the authors. This contrast aids in the detection of the disease named glaucoma, which occurs in the retina.

Table 1: Comparison on various techniques presented by the authors

Study	Preprocessing Techniques	Segmentation Model	Retinal Structures Targeted	Evaluation Metrics	Key Findings
Gegundez-Arias et al. (2021)	Retinal Image Enhancement	Modified U-Net Model	Retinal Blood Vessels	Sensitivity, Specificity	Demonstrated superior performance on retinal vessel segmentation.
Li et al. (2022)	Defaced Image Denoising	DAC-CLGD-Danet Network	General Image Segmentation	Precision, Recall	Effective segmentation despite challenging image conditions.
Alsayat et al. (2023)	Multi-Layer Preprocessing	U-Net with Residual Attention Block	Retinal Blood Vessels	Dice Coefficient, Sensitivity, Specificity	Improved segmentation accuracy through residual attention.
Wen et al. (2024)	Image Denoising Techniques	Transformer-Assisted Cascade Learning Network	Choroidal Vessels	Dice Coefficient, Intersection over Union	Demonstrated accurate choroidal vessel segmentation.
Wong et al. (2024)	Semi-Supervised Preprocessing	Cross-Teaching CNN + Transformer Integration	Volumetric Segmentation in OCT	Dice Similarity Coefficient	Achieved enhanced segmentation using semi-supervised frameworks.

3. PROPOSED METHODOLOGY

This paper aims to detect the glaucoma disease in retinal images. For this detection, two algorithms are proposed based on its detecting capabilities. The former one is Adaptive Noise Elimination Neural Network (ANENN). This method is used for image Denoising; the inputted image is denoised by removing the noise for the accurate detection of glaucoma. The latter one is Improved Mask Region-based Convolutional Neural Networks (Mask R-CNN). This approach is exploited for image segmentation. The fed image is segmented and categorized based on the diseased area. Thus, these two methods aid in accurate glaucoma

detection, leading to the earliest recovery of the glaucoma patients.

Image Denoising Using Adaptive Noise Elimination Neural Network in Glaucoma Detection

Globally, glaucoma refers to a disorder which gradually impairs the optic nerve. This is the leading cause of permanent blindness. Earlier detection and diagnosis of the disease assist to in avoiding blindness. Fundus photography and OCT are the most essential imaging tools for diagnosing glaucoma. Noise generated during the acquisition process make it difficult for the diagnostic equipment to detect the images with accuracy. Therefore, efficient denoising of these images is critical to ensure high-quality inputs in the following diagnostic assessment.

While dealing with noisy medical images, few denoising algorithms like wavelet transform and Gaussian smoothing struggle to preserve the external structures and minute information. In this paper, ANENN is designed specifically for denoising the glaucoma images as well as provide the solution to the raised problems. This model keeps the necessary detected information by learning to discriminate between background noise and indeed image features.

Adaptive Noise Elimination Neural Network model functions on DL and adaptive filtering. A noise estimation module is incorporated in the model, which continuously explores the type and degree of image noise. This estimate directs the Convolutional Neural Network (CNN) to apply denoising in the specified regions. During the elimination of unwanted noise, key components regarding the retinal nerve fiber layer, optic nerve head and macula are protected. Network adaptability assures that the performance remains constant over varied imaging technique regardless of the different background noise levels.

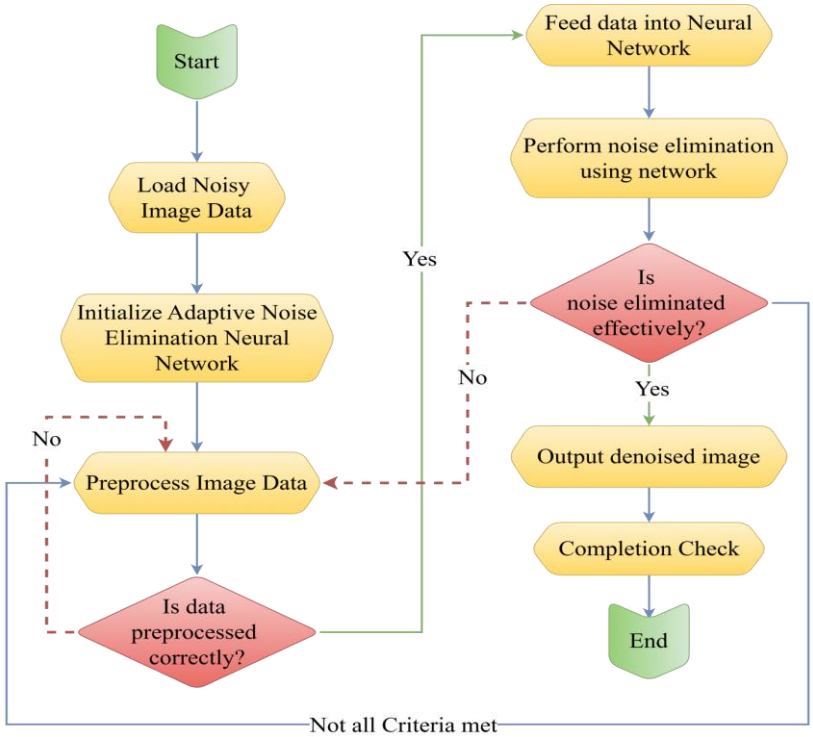

Figure 2: ANENN utility for image-denoising

Figure 2 depicts ANENN working as a flow diagram in images. The procedure begins with preprocessing the noisy pictures, which is followed by noise removal using a neural network. We iteratively test the accuracy of the preprocessing and the efficiency of the reduction.

High-resolution along with noise-free images are required for operations such as optic disc and cup segmentation, disc-to-cup ratio computation and nerve fiber layer thinning analysis. These effectively recognize glaucoma. In ANENN framework, image clearance and feature recognition is increased, which further enhances the disease detection. Signal-to-noise ratio (SNR) and peak signal-to-noise ratio (PSNR) are increased for quantitative studies in qualitative assessments. This examination provides a more complete view of images.

High-resolution along with noise-free images are required for operations such as optic disc and cup segmentation, disc-to-cup ratio computation and nerve fiber layer thinning analysis. These effectively recognize glaucoma. In ANENN framework, image clearance and feature recognition is increased, which further enhances the disease detection. Signal-to-noise ratio (SNR) and peak signal-to-noise ratio (PSNR) are increased for quantitative studies in qualitative assessments. This examination provides a more complete view of images.

Algorithm 1: Adaptive Noise Elimination Neural Network Algorithm

Input:

Retinal image is trained to distinguish the noise by using a noisy input grayscale image (input_image); a threshold is utilized for recognizing noise (threshold) and window size determines the adaptive filtering window (window_size).

Procedure:

1.Scan the image:

Feed the image (input_image), which is grayscale with some noise.

2. Describe a sliding window.

Use a 3x3 or 5x5 square sliding window (window_size), which matches the window size exactly.

3. Calculate common statistics:

Identify the neighborhoods in the window that are centered on each image pixel. Determine the window's average and variance of pixel values.

Repeat the process for every pixel in the image.

4. Adjust to local noise:

If the local variance is lower than a predefined (threshold), the pixel value remains unchanged; it indicates the low noise levels.

If the local variance is excess than the (threshold), the pixel value has to be replaced with the local average value for removing noise.

5. Repetition:

Applying the above mentioned adaptive rule , sliding window is adjusted over the whole image.

6. Image preservation:

The image has to be preserved and exhibited.

Output:

An image which is denoised (denoised_image).

Algorithm 1 describe Adaptive Noise Elimination Neural Network algorithm. This method process the input image to reduce noise while preserving the important features relevant to glaucoma detection, such as edges and texture details.

The proposed ANENN gives clear inputs, which improves the sensitivity and specificity in the glaucoma detection. Thus, it increases the effectiveness of automated diagnosis systems. As a consequence, important improvements are achieved in medical image processing and serve as the base for the highly accurate, noninvasive glaucoma treatment diagnostic technologies.

Adaptive Noise Eliminating Neural Network gives high accurate glaucoma identification through the offering of robust and proper solution to the noisy medical imaging issue. During the noise removal, storing the clinically associated information is assured. This, in turn, enables the Oculist to make quick and exact diagnoses. Thereby, outcomes of the patient are increased. Equation (1) determines the noise level in the inputted image:

$$I_{noisy}(x,y) = I_{signal}(x,y) + N(x,y) \text{ ---------- (1)}$$

The noisy input image $I_{noisy}(x,y)$, obtained by imaging systems, is defined by the pixel coordinates x and y. This image depicts the actual external features along with the unnecessary noise. The primary clear signal $I_{signal}(x,y)$, indicates the actual external structure of eye like the layers of retina and the optic nerve head. Noise represented in the image as N (x, y), is from image acquisition. This nose includes the sensor and surrounding requirements accompanied with the random distortions. Equation (2) gives an estimation of adaptive noise.

$$N_{adaptive}(x,y) = f_{ANENN}\left(I_{noisy}(x,y)\right) \text{ ---------- (2)}$$

$N_{adaptive}(x,y)$ represents the ANENN's computed noise component with adaptation. The functional representation for ANENN is $f_{ANENN}\left(I_{noisy}(x,y)\right)$. Regarding $I_{noisy}(x,y)$, noise characteristics are acquired depending on the local and global image features. Equation (3) quantifies the denoised image.

$$I_{denoised}(x,y) = I_{noisy}(x,y) - N_{adaptive}(x,y) \text{ ---------- (3)}$$

$I_{denoised}(x,y))$ is the output image obtained after removing the adaptive noise component $N_{adaptive}(x,y)$ and holds only the clean signal $I_{signal}(x,y)$.

Segmentation Using Improved Mask R-CNN in Glaucoma Detection

Globally, glaucoma is the leading cause of permanent blindness, mostly affecting the optic nerve. Examining the Optic Disc (OD) and Optic Cup (OC) boundaries in retinal fundus images reveals CDR. This significantly controls this degenerative disease. Earlier detection is the key for effective disease management. Only if these structures are effectively segregated, reliable CDR measurement helps in prior glaucoma identification. Mask R-CNN, with its high

accuracy in instance segmentation, has gained popularity in medical imaging as an example of the potential of DL-based automated segmentation algorithms. As retinal images are inherently diverse and irregular, the traditional Mask R-CNN approach frequently overlooks the challenges in glaucoma detection.

Improved Mask R-CNN integrates the instance segmentation, object identification and classification throughout a single approach. The model is excellent candidate for automating glaucoma detection segmentation activities because it separates the key components such as OD and OC. However, a variety of unique obstacles including less contrast, changing illumination and subtle discrimination betwixt glaucomatous and healthy eyes are provided by retinal images. In order to deal with these problems, Mask R-CNN design has been improved in variety of ways for increasing its reliability and effectiveness in detecting glaucoma.

Preprocessing is one of the most essential enhancements to improve the quality of retinal images. Gaussian smoothing and Contrast-Limited Adaptive Histogram Equalization (CLAHE) techniques are utilized for illumination normalization along with the increase in contrast. This makes the OD and OC unique. Improved Mask R-CNN's backbone network facilitates the creation of sophisticated designs such as EfficientNet and DenseNet by retrieving features from input pictures. While enhancing feature extraction, these networks retain their computational efficiency. Training the model with Feature Pyramid Network (FPN) increases its image identification capabilities at several levels, allowing for effective segmentation of optic nerve head in images with varying resolutions.

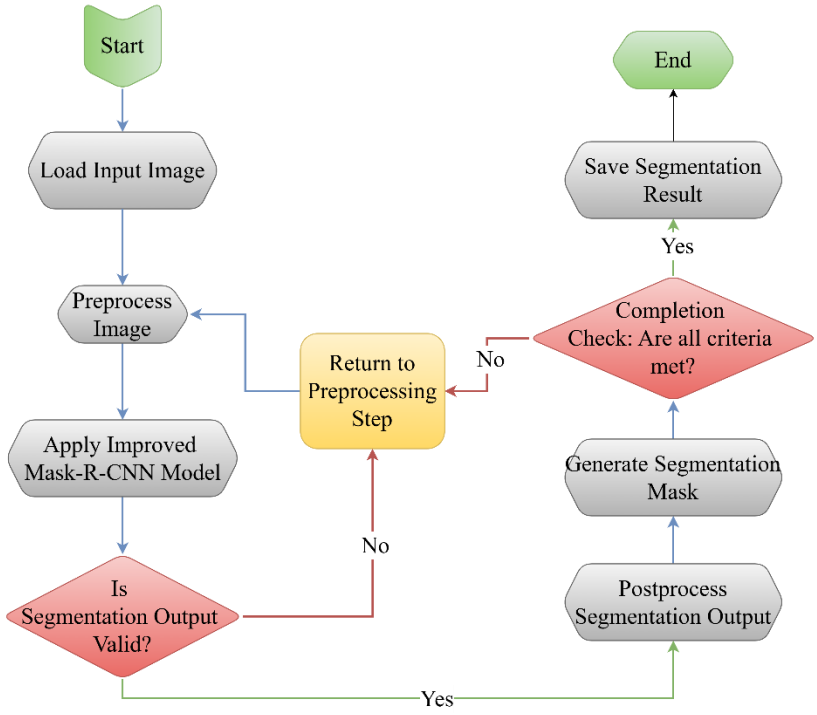

Figure 3: Exploitation of improved Mask -RCNN for segmentation

The visual representation in figure 3 is segmented using an improved Mask-RCNN

model. Image preprocessing, segmentation validation, mask generation, and post processing are all iterative refinement loops that ensure all requirements are met throughout the process.

Customized training helps to increase segmentation accuracy. Domain-relevant image augmentation techniques including rotating, scaling and varying the brightness is used to ensure the model performance with various sorts of image. Moreover, changing the weights of OD and OC boundaries in loss function improves the segmentation accuracy better. Post-processing methods like contour smoothing and morphological operations help to guarantee appropriate delineation of these important characteristics. Hence, optimizing segmentation helps in the reduction of noise.

Algorithm 2: Improved Mask R-CNN algorithm

Input:

A grayscale fundus image (input_image) as input has to be first preprocessed.

A base point (base_x,base_y) points the locations like OD centre.

A threshold (threshold) is a minimal value, which represents the degree of similarity between intensities.

1. Initialization

Set the starting points (base_x, base_y) for the area to partition.
First, construct a segmented image or binary mask and then add a zero value.

2. Region Growing

Add the base point to the waiting image.

Remove one, even if the queue still has pixels:
Set the current pixel intensity to its original base point.

If the intensity difference is less than or equal to threshold, indicate that the pixel is a part of segmented picture region.

3. Halt the condition:

When every connected pixel in the intensity range is within the area, the process ends.

4. Post-Processing

Morphological operations such as erosion and dilation is implied to alter the segmented region.

5. Display of image

Save the image that highlights the segmented region.

Output:

The final input is a segmented binary image (segmented_image), with an highlighted disease area.

Algorithm 2 indicates the Improved Mask R-CNN architecture. It begins by using morphological techniques to refine the findings before stretching a region from a starting point to embrace surrounding pixels with an intensity threshold, resulting in the segmentation of a grayscale fundus image. The final result is a binary image with the highlight diseased area.

Including clinical parameters like Intra Ocular Pressure (IOP) and visual field test results increase the segmentation performance and diagnostic reliability of improved Mask R-CNN models. Large, diverse datasets has to be evaluated on the model to assure its effectiveness in clinical settings. These enhancements aid in properly segmenting OD and OC using an updated Mask R-CNN framework. Hence, earlier glaucoma detection is boosted. This technique accelerates the detection process and improves patient outcomes by providing a prompt and accurate report. The segmentation emphasize on loss function analysis. The loss function is calculated as;

$$L = L_{cls} + L_{bbox} + L_{mask} \text{ --------- (4)}$$

Equation (4) shows that the total loss function L is included in Mask R-CNN training equation. L_{cls}, L_{bbox} and L_{mask} are the inscription of three losses: mask loss, bounding box regression loss and classification loss, respectively. Mask loss is determined using the formula in the following equation (5).

$$L_{mask} = \frac{1}{N} \sum_{i-1}^{N} \left[y_i \log\left(\hat{Y}\right) + (1 - y_i) \log\left(1 - \hat{Y}\right) \right] \text{ ---------- (5)}$$

Equation (5) includes the ground truth binary label for pixel i, predicted probability of pixel i, the natural logarithm, mask loss and the mask's pixel count, which are denoted in the form of the variables such as y_i, $\hat{Y}, \log, L_{mask}$ and N. In contrast, equation (6) yields CDR.

$$CDR = \frac{A_{cup}}{A_{disc}} \text{ ---------- (6)}$$

The pixel areas of OC and OD are A_{cup} andA_{disc}. Therefore, in equation (7) Intersection over Union (IoU) for segmentation accuracy is estimated as.

$$IoU = \frac{| M_{true} \cap M_{pred} |}{| M_{true} \cup M_{pred} |} \text{ ---------- (7)}$$

M_{true} is the ground truth mask, while M_{pred} refers to the projected mask calculated by the application of the models to estimate the mask for a specific area, such as OC or OD. The symbol |.| represents the cardinality of pixel set. ∩ and ∪ refers to the common and the total pixels betwixt M_{true} and M_{pred}, respectively.

$$Dice = \frac{2 | M_{true} \cap M_{pred} |}{| M_{true}| + | M_{pred} |} \text{ ---------- (8)}$$

Dice Coefficient is commonly used in image segmentation applications such as medical imaging for glaucoma diagnosis, as shown in equation (8). Comparing the ground truth mask (M_{true}) and the expected mask (M_{pred}), the similarities are calculated

4. RESULTS AND CONCLUSION

The suggested Adaptive Noise Elimination Neural Network (ANENN) is a lot better than PSNR-based retinal image denoising (34.5), SSIM (0.92), and RMSE (3.8) and is much better compared to conventional techniques like DWT, GAN, NLM, and NLW. This makes the retinal images clearer and acceptable for further processing. The improved Mask R-CNN model for segmentation achieved 96.1% accuracy, 95.0% precision, 95.3% recall, and 94.7%

F-measure, much improved compared to methods such as Watershed Segmentation, FCM, and FCN. The improved model also achieves accurate estimation of Cup-to-Disc Ratio (CDR), an important key to the diagnosis of glaucoma. All these promote more accurate and automated detection of glaucoma, enabling possible earlier and appropriate diagnosis. The pairing of ANENN for noise removal and the improved Mask R-CNN for segmentation forms a robust system for glaucoma detection. Both these approaches provide significant improvements in automated ophthalmic diagnosis, resulting in early treatment and avoiding intractable vision loss.

4.1 Performance metrics

4.1.1 Peak Signal-to-Noise Ratio (PSNR):

$$\text{PSNR} = 10\log_{10}\left(\frac{(L_{max})^2}{\text{MSE}}\right) \text{ -------- (9)}$$

Where, L_{max} is the maximum possible pixel value. Higher PSNR indicates better denoising quality of leaf image. Equation 9 PSNR quantifies the quality of the denoised image by measuring how much the denoised image deviates from the clean image.

4.1.2 Structural Similarity Index (SSIM):

$$\text{SSIM} = \frac{(2\mu_x\mu_y+C_1)(\sigma_{xy}+C_2)}{(\mu_x^2+\mu_y^2+C_1)(\sigma_x^2+\sigma_y^2+C_2)} \text{ ---------- (10)}$$

Equation 10 measures structural similarity between the clean and denoised images. SSIM compares the structural information (contrast, luminance, and texture) between the clean and denoised damaged leaf images. Unlike PSNR, which only considers pixel differences, SSIM evaluates how well the structure and details are preserved. A value close to 1 indicates high similarity, meaning better denoising performance.

4.1.3 Root Mean Squared Error (RMSE):

$$\text{RMSE} = \sqrt{\text{MSE}} \text{ ---------- (11)}$$

In equation 11 lower RMSE values indicate better denoising performance. RMSE measures the overall pixel-wise error between the denoised and ground truth leaf images. A lower RMSE value indicates a better denoised image with fewer distortions.

4.1.4 Accuracy

$$\text{Accuracy} = \frac{\text{TP+TN}}{\text{TP+TN+FP+FN}} \text{ ------- (12)}$$

T-True, F-False, P-Positive, N-Negative

In predictive modeling, accuracy is the measure of closest model's projections is to real-world outcomes. Equation 12 evaluates the model because many choices and forecasts rely on its accuracy and dependability.

4.1.5 Precision

$$\text{Precision} = \frac{\text{TP}}{\text{TP+FP}} \text{ ------ (13)}$$

Equation 13 predictive modeling, accuracy is the proportion of total expected positive

observations to correctly forecast positive observations it demonstrates the model's successful reduction of false positives, guaranteeing that the positive forecasts it delivered are accurate and reliable by extension and error reduction in many other domains.

4.1.6 Recall

$$\text{Recall} = \frac{\text{TP}}{\text{TP+FN}} \text{ ------ (14)}$$

Equation 14 predictive modeling is the fraction of real positive instances properly detected in the model. In sectors like identifying all positives is critical since it shows the efficient detection of all relevant instances in a particular class.

4.1.7 F-measure

$$\text{F} - \text{measure} = 2 \times \frac{\text{Precision} \times \text{recall}}{\text{precision+recall}} \text{ ------- (15)}$$

Equation 15, which determines the harmonic mean of recall and accuracy, is a strong all-around measurement of the efficient performance in model that is necessary for preventing both false positives and false negatives.

Table 2: Comparison table for Denoising

Algorithms/Metrics	PSNR	SSIM	RMSE
DWT	28.5	0.82	6.8
GAN	32.1	0.88	4.9
NLM	29.7	0.85	6.1
NLW	31.3	0.87	5.2
ANENN (Proposed)	34.5	0.92	3.8

Table 2 shows comparison of various denoising algorithms for glaucoma detection in terms of PSNR, SSIM, and RMSE. The Proposed ANENN model performs better than the conventional methods with the best PSNR (34.5 dB), which reflects better noise removal and image quality. Its SSIM (0.92) reflects better preservation of structural detail than Generative Adversarial Network (GAN), Non Local Means (NLM), and Non Local wavelet (NLW) methods. The RMSE (3.8) is also lowest, reflecting less reconstruction error and better image quality. This implies that ANENN has the capability of eliminating noise without losing significant diagnostic characteristics and therefore more suited to medical imaging purposes.

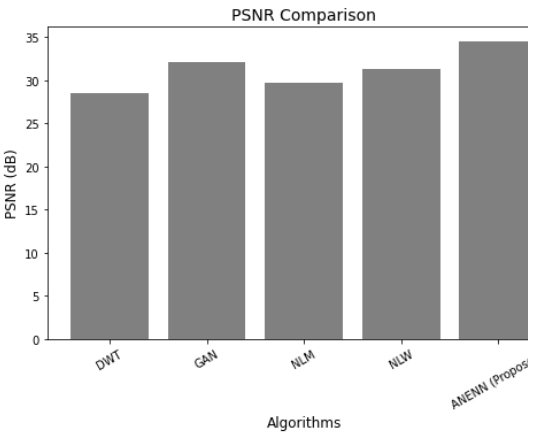

Figure 4: Comparison chart of PSNR

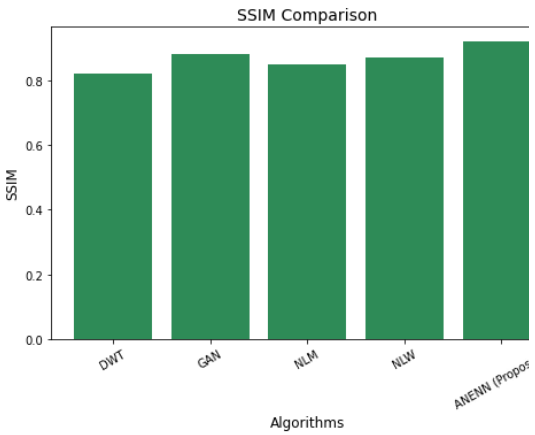

Figure 5: Comparison chart of SSIM

Figure 4 displays that the proposed ANENN algorithm has the maximum PSNR value, meaning it provides better quality images and suppressed noise. In this chart the x-axis shows the denoising algorithms and the y-axis shows the PSNR values.

Figure 5 displays the SSIM values of denoising algorithms such as Discrete Wavelet Transform (DWT), GAN, NLM, NLW and proposed ANENN. In this chart the x-axis shows the denoising algorithms and the y-axis shows the SSIM values.

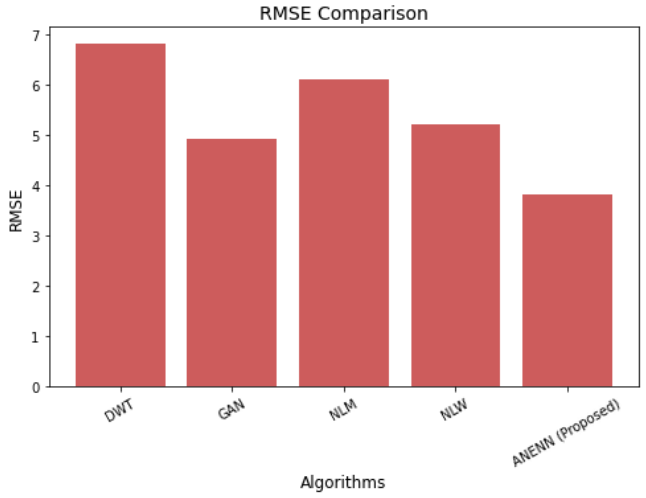

Figure 6: Comparison chart of RMSE

Figure 6 displays the RMSE values of denoising algorithms such as DWT, GAN, NLM, NLW and proposed ANENN. In this chart the x-axis shows the denoising algorithms and the y-axis shows the RMSE values.

Table 3: Comparison table for Segmentation

Algorithms/ Metrics	Accuracy	Precision	Recall	F-measure
Watershed Segmentation	85.4	83.4	84.7	82.1
FCM	88.2	86.2	86.9	85.6
FCN	91.5	90.0	90.8	89.3
RCNN	93.2	92.1	92.5	91.8
Improves Mask-RCNN	96.1	95.0	95.3	94.7

Table 3 compares the performance of various image segmentation algorithms in terms of accuracy, precision, recall, and F-measure. Watershed Segmentation has moderate performance with 85.4% accuracy and low F-measure (82.1%), which means that it might leave out some true positives. FCM (Fuzzy C-Means) and FCN (Fully Convolutional Network) improve the performance, and FCN has 91.5% accuracy with precision and recall in equilibrium. RCNN even better optimizes the performance to 93.2% accuracy with precision and recall of close to 92%. Mask-RCNN improved is the best among all with the highest accuracy of 96.1% and balanced values, showing enhanced segmentation performance.

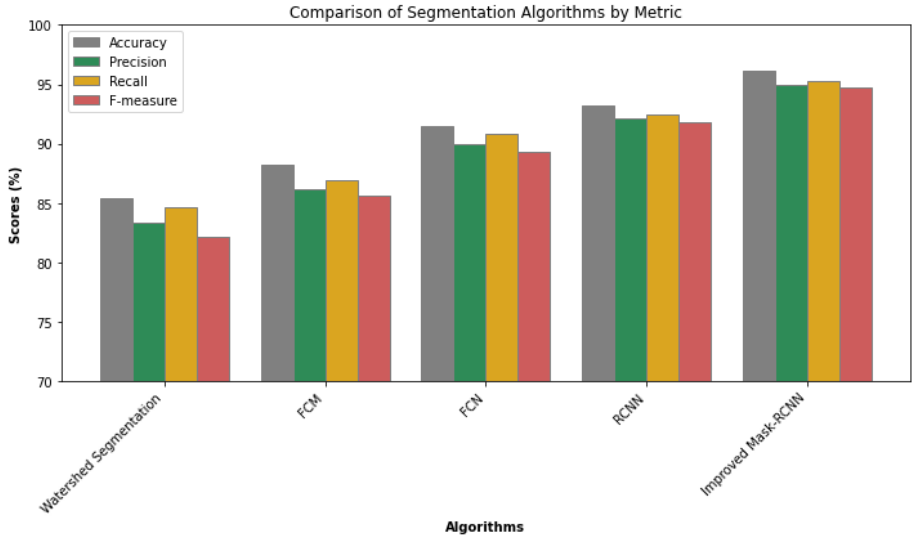

Figure 7: Comparison chart of performance metrics

Figure 7 illustrates the comparison of accuracy, precision, recall and f-measure for various algorithms such as, Watershed Segmentation, FCM, FCN, RCNN, improved Mask-RCNN. In this chart the x-axis shows the segmentation algorithms and y-axis shows the metric scores.

5. CONCLUSION

The Proposed Methodology uses improved Mask-R-CNN for segmentation and image denoising with ANENN. These methods provide a significant solution for retinal image processing in glaucoma diagnosis technique. The noise removal capability of ANENN

increases the retinal image quality for segmentation. Improved Mask-R-CNN segments the two critical components for glaucoma identification such as the optic disc and cup. The system's ability to detect glaucoma is enhanced by incorporating the variety of strategies that improves the overall accuracy of feature extraction. This technique not only ensures robustness regardless of image quality and facilitates early diagnosis through the use of a segmentation algorithm. Denoising and segmentation improve the automated glaucoma detection. These algorithms are refined for future usage in clinical situations with diverse retinal images. This strategy lowers the burden of manual diagnosis and helps in the ease treatment of glaucoma patients.

References

1. Shalini, R., & Gopi, V. P. (2024). Multiresolution cascaded attention U-Net for localization and segmentation of optic disc and fovea in fundus images. Scientific Reports, 14(1), 23107.
2. Hassan, B., Qin, S., Hassan, T., Akram, M. U., Ahmed, R., & Werghi, N. (2021). CDC-Net: Cascaded decoupled convolutional network for lesion-assisted detection and grading of retinopathy using optical coherence tomography (OCT) scans. Biomedical Signal Processing and Control, 70, 103030.
3. Kang, S., Iwana, B. K., & Uchida, S. (2021). Complex image processing with less data—Document image binarization by integrating multiple pre-trained U-Net modules. Pattern Recognition, 109, 107577.
4. Lian, S., Li, L., Lian, G., Xiao, X., Luo, Z., & Li, S. (2019). A global and local enhanced residual u-net for accurate retinal vessel segmentation. IEEE/ACM transactions on computational biology and bioinformatics, 18(3), 852-862.
5. Zhang, Y., Li, Z., Nan, N., & Wang, X. (2023). TranSegNet: hybrid CNN-vision transformers encoder for retina segmentation of optical coherence tomography. Life, 13(4), 976.
6. Aurangzeb, K., Alharthi, R. S., Haider, S. I., & Alhussein, M. (2023). Systematic development of AI-Enabled diagnostic systems for glaucoma and diabetic retinopathy. IEEE Access, 11, 105069-105081.
7. Yu, Y., & Zhu, H. (2023). M3U-CDVAE: Lightweight retinal vessel segmentation and refinement network. Biomedical Signal Processing and Control, 79, 104113.
8. Mehmood, M., Alsharari, M., Iqbal, S., Spence, I., & Fahim, M. (2024). RetinaLiteNet: A Lightweight Transformer based CNN for Retinal Feature Segmentation. In Proceedings of the IEEE/CVF Conference on Computer Vision and Pattern Recognition (pp. 2454-2463).
9. Alsayat, A., Elmezain, M., Alanazi, S., Alruily, M., Mostafa, A. M., & Said, W. (2023). Multi-Layer Preprocessing and U-Net with Residual Attention Block for Retinal Blood Vessel Segmentation. Diagnostics, 13(21), 3364.
10. Gegundez-Arias, M. E., Marin-Santos, D., Perez-Borrero, I., & Vasallo-Vazquez, M. J. (2021). A new deep learning method for blood vessel segmentation in retinal images based on convolutional kernels and modified U-Net model. Computer Methods and Programs in Biomedicine, 205, 106081.
11. Goutam, B., Hashmi, M. F., Geem, Z. W., & Bokde, N. D. (2022). A comprehensive review of deep learning strategies in retinal disease diagnosis using fundus images. IEEE Access, 10, 57796-57823.
12. Wong, D., Sreng, S., Phuong, P. D. N., Gani, N. F. B. A., Chua, J., Nongpiur, M. E., ... & Ramesh, P. (2024). Enhancing Volumetric Segmentation in Wide-Field OCT Images with a Semi-Supervised Learning Framework: Cross-Teaching CNN and Transformer Integration.
13. Wen, Y., Wu, Y. L., Bi, L., Shi, W. Z., Liu, X. X., Xu, Y. P., ... & Feng, D. D. (2024). A Transformer-Assisted Cascade Learning Network for Choroidal Vessel Segmentation. Journal

of Computer Science and Technology, 39(2), 286-304.
14. Li, P., Li, G., He, Y., Zhang, L., Sun, Y., & Guo, F. (2022). A DAC-CLGD-Danet network based method for defaced image segmentation. Intelligent and Converged Networks, 3(3), 294-308.
15. Wang, J., Li, X., Lv, P., & Shi, C. (2021). SERR-U-Net: Squeeze-and-Excitation Residual and Recurrent Block-Based U-Net for Automatic Vessel Segmentation in Retinal Image. Computational and Mathematical Methods in Medicine, 2021(1), 5976097.
16. Peng, L., Lin, L., Cheng, P., Wang, Z., & Tang, X. (2021). Fargo: A joint framework for faz and rv segmentation from octa images. In Ophthalmic Medical Image Analysis: 8th International Workshop, OMIA 2021, Held in Conjunction with MICCAI 2021, Strasbourg, France, September 27, 2021, Proceedings 8 (pp. 42-51). Springer International Publishing.
17. Karn, P. K., & Abdulla, W. H. (2023). On machine learning in clinical interpretation of retinal diseases using oct images. Bioengineering, 10(4), 407.
18. Devalla, S. K., Pham, T. H., Panda, S. K., Zhang, L., Subramanian, G., Swaminathan, A., ... & Girard, M. J. (2020). Towards label-free 3D segmentation of optical coherence tomography images of the optic nerve head using deep learning. Biomedical optics express, 11(11), 6356-6378.
19. Wang, J., Chen, C., Li, F., Wang, Z., Qu, G., Qiao, Y., ... & Zhang, X. (2018). SD Net: joint segmentation and diagnosis revealing the diagnostic significance of using entire RNFL thickness in glaucoma.
20. Kar, M. K., Nath, M. K., & Neog, D. R. (2021). A review on progress in semantic image segmentation and its application to medical images. SN computer science, 2(5), 397.